Transition of responsive mechanosensitive elements from focal adhesions to adherens junctions on epithelial differentiation

Barbara Noethel[a], Lena Ramms[a], Georg Dreissen[a], Marco Hoffmann[a], Ronald Springer[a], Matthias Rübsam[b], Wolfgang H. Ziegler[c], Carien M. Niessen[b], Rudolf Merkel[a], and Bernd Hoffmann[a,*]

[a]Forschungszentrum Jülich, Institute of Complex Systems, ICS-7: Biomechanics, 52428 Jülich, Germany; [b]Department of Dermatology, Cologne Excellence Cluster on Cellular Stress Responses in Aging-Associated Diseases (CECAD), Center for Molecular Medicine Cologne, University of Cologne, 50931 Cologne, Germany; [c]Department of Pediatric Kidney, Liver and Metabolic Diseases, Hannover Medical School, 30625 Hannover, Germany

ABSTRACT **The skin's epidermis is a multilayered epithelial tissue and the first line of defense against mechanical stress. Its barrier function depends on an integrated assembly and reorganization of cell–matrix and cell–cell junctions in the basal layer and on different intercellular junctions in suprabasal layers. However, how mechanical stress is recognized and which adhesive and cytoskeletal components are involved are poorly understood. Here, we subjected keratinocytes to cyclic stress in the presence or absence of intercellular junctions. Both states not only recognized but also responded to strain by reorienting actin filaments perpendicular to the applied force. Using different keratinocyte mutant strains that altered the mechanical link of the actin cytoskeleton to either cell–matrix or cell–cell junctions, we show that not only focal adhesions but also adherens junctions function as mechanosensitive elements in response to cyclic strain. Loss of paxillin or talin impaired focal adhesion formation and only affected mechanosensitivity in the absence but not presence of intercellular junctions. Further analysis revealed the adherens junction protein α-catenin as a main mechanosensor, with greatest sensitivity conferred on binding to vinculin. Our data reveal a mechanosensitive transition from cell–matrix to cell–cell adhesions on formation of keratinocyte monolayers with vinculin and α-catenin as vital players.**

Monitoring Editor
Alpha Yap
University of Queensland

Received: Jun 19, 2017
Revised: Jul 12, 2018
Accepted: Jul 17, 2018

INTRODUCTION

The epidermal skin barrier is essential to protect the organism from external factors while being permanently affected by mechanical stress (Sanders *et al.*, 1995; Chuong *et al.*, 2002). To ensure tissue integrity and proper barrier function, this self-renewing, multilayered epithelium dynamically organizes specialized cell–matrix and cell–cell junctions in a layer-dependent manner (Simpson *et al.*, 2011). With focal adhesions (FAs) cell–matrix adhesions are present in the basal epidermal layer to connect the extracellular basement membrane with the actin cytoskeleton. Furthermore, adherens junctions (AJs) are formed as intercellular contacts. Here, classical cadherins interact through β-catenin and α-catenin (Vasioukhin *et al.*, 2000) to actin (Rudiger, 1998). Initiation of differentiation induces upward movement of keratinocytes into the first suprabasal layer, resulting in loss of FAs while at the same time reorganizing and potentially strengthening AJs (Eckert, 1989; Simpson *et al.*, 2011; Rubsam *et al.*, 2017; Miroshnikova *et al.*, 2018). As cadherins are Ca^{2+}-dependent adhesion molecules, intercellular contact formation and differentiation of epithelia can be mimicked in vitro by switching cells to high levels of calcium (O'Keefe *et al.*, 1987; Fuchs, 1990; Vaezi *et al.*, 2002).

Owing to permanent exposure of the skin to mechanical stimuli, mechanosensoric proteins perceive the mechanical signal and induce cellular responses within the epidermis to adapt to such impacts. Various mechanisms for mechanosensation have been described. One of them is strain-induced conformational

This article was published online ahead of print in MBoC in Press (http://www.molbiolcell.org/cgi/doi/10.1091/mbc.E17-06-0387) on July 25, 2018.

*Address correspondence to: Bernd Hoffmann (b.hoffmann@fz-juelich.de).

Abbreviations used: AJ, adherens junction; Ecad, E-cadherin; FA, focal adhesion; KO, knockout; Pax, paxillin; Pcad, P-cadherin; Tln, talin; Vinc, vinculin; WT, wild type.

changes of proteins leading to exposure of hidden domains (Bakolitsa *et al.*, 2004; Yonemura *et al.*, 2010; Twiss and de Rooij, 2013). For AJs, conformational changes in α-catenin have been shown on force application (Yonemura *et al.*, 2010; Twiss and de Rooij, 2013; Yao *et al.*, 2014). For FAs several of such proteins have been described, with tension-dependent conformational opening of talin and subsequent binding to integrins and actin mentioned just as an example (del Rio *et al.*, 2009).

One vital response to strain is the reorientation of actin bundles within the cell (Hayakawa *et al.*, 2000; Wang *et al.*, 2001; Neidlinger-Wilke *et al.*, 2002). Above a certain threshold in stretch amplitude and frequency, stress fibers reorient away from the direction of strain to maintain mechanical homeostasis (Hayakawa *et al.*, 2000, 2001; Wang *et al.*, 2001; Jungbauer *et al.*, 2008). However, until now almost all experiments on cellular strain response have been performed on the single-cell level, leading to the identification of mainly FA bound mechnosensoric proteins, e.g., vinculin or p130 Cas (Sawada *et al.*, 2006). In contrast, very little is known on strain-induced cytoskeletal reorientation processes in epithelial monolayers that are connected by cell–cell contacts. Interestingly, vinculin is recruited not only to FAs but also to AJs on formation (Twiss and de Rooij, 2013). In AJs interaction takes place via direct binding to α-catenin in a tension-dependent manner (Yonemura *et al.*, 2010). This interaction is then thought to locally reorganize actomyosin resulting in junctional strengthening (Huveneers *et al.*, 2012). Furthermore, on formation of epithelial cell sheets, FAs reorganize with vinculin largely lost from FAs (Opas *et al.*, 1985; Herman *et al.*, 1986; O'Keefe *et al.*, 1987; Hodivala and Watt, 1994; Braga *et al.*, 2009; Mertz *et al.*, 2013).

Here, we have analyzed and compared the cellular response to cyclic strain of a keratinocyte monolayer in low calcium conditions thus permitting only cell–matrix adhesions with the response of a monolayer of cells allowed to form cell–cell contacts and to initiate early differentiation. Our results reveal the presence of two independent mechanosensitive complexes for actin reorientation: FAs for cells without cell–cell contacts, and AJs as a central mechanoresponsive element in calcium-induced early-stage differentiated epidermal cells. Moreover, we provide evidence that together with its binding partner vinculin, α-catenin acts as a mechanosensor in this complex, which on initiation of intercellular adhesion enables a transition process in which the mechanical control of actin reorganizations is transferred from focal adhesions to adherens junctions.

RESULTS

Intercellular contacts reinforce strain-induced stress fiber reorientation

To address whether initiation of intercellular contact formation and differentiation would affect cytoskeletal reorientation in response to cyclic stretch, keratinocyte monolayers were either allowed (high calcium) or not allowed (low calcium) to initiate intercellular junction formation for 2 h and then subjected to cyclic stretch for 4 h under the same calcium conditions and compared with unstretched control cells (Figure 1). Quantitative orientation analyses of actin stress fibers revealed a significant difference between cells that were cyclically stretched in the presence of calcium and those that were kept in low calcium media (Figure 1E). In both experiments, stress fibers oriented away from the direction of stretch, albeit more extensively in high calcium media, with almost all fibers being in a range between 30° and 90° with low calcium and 60° and 90° with high calcium. Thus, cells allowed to form intercellular contacts reinforce external stress-induced reorientation of the actin cytoskeleton.

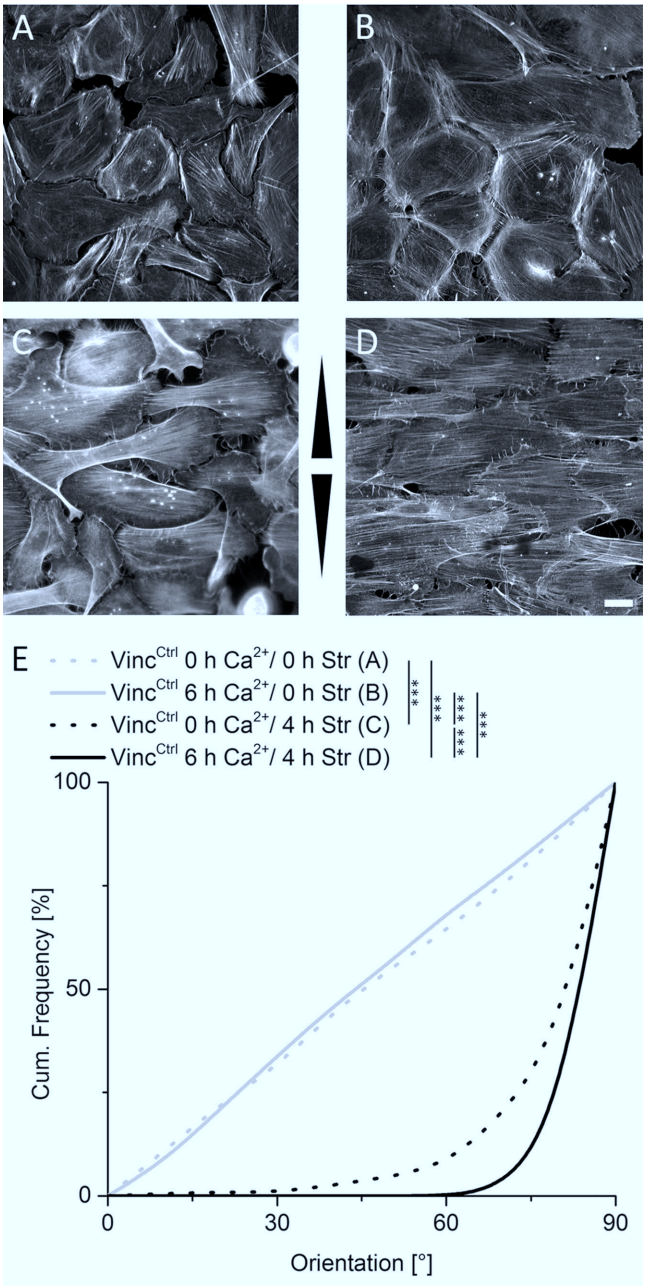

FIGURE 1: Induction of intercellular junction formation positively affects actin reorientation. Control cells were grown in the absence (A, C) and presence (B, D) of calcium to induce intercellular junction formation and subjected to 4 h of cyclic stretch (C, D). Arrowheads indicate stretch direction. Scale bar 20 μm. After fixation and staining of actin filaments, angular distributions were plotted as cumulative histogram with 0° corresponding to strain direction and 90° perpendicular to it (E) ($n_A = 157$, $n_B = 284$, $n_C = 416$, and $n_D = 402$).

Strain enhances FA loss in epithelial sheets

On the basis of positive control analyses for the experimental setup according to Twiss and de Rooij (2013), we were also able to detect the switch of vinculin from FAs to AJs, slightly reduced numbers of FAs, and actin cytoskeletal cortical ring formation in the presence of 6 h of Ca^{2+} (Supplemental Figure 2). We next tested whether cyclic strain would affect vinculin, paxillin, and F-actin localization under high calcium. Applying external force decreased cell coverage of paxillin-labeled FAs significantly by

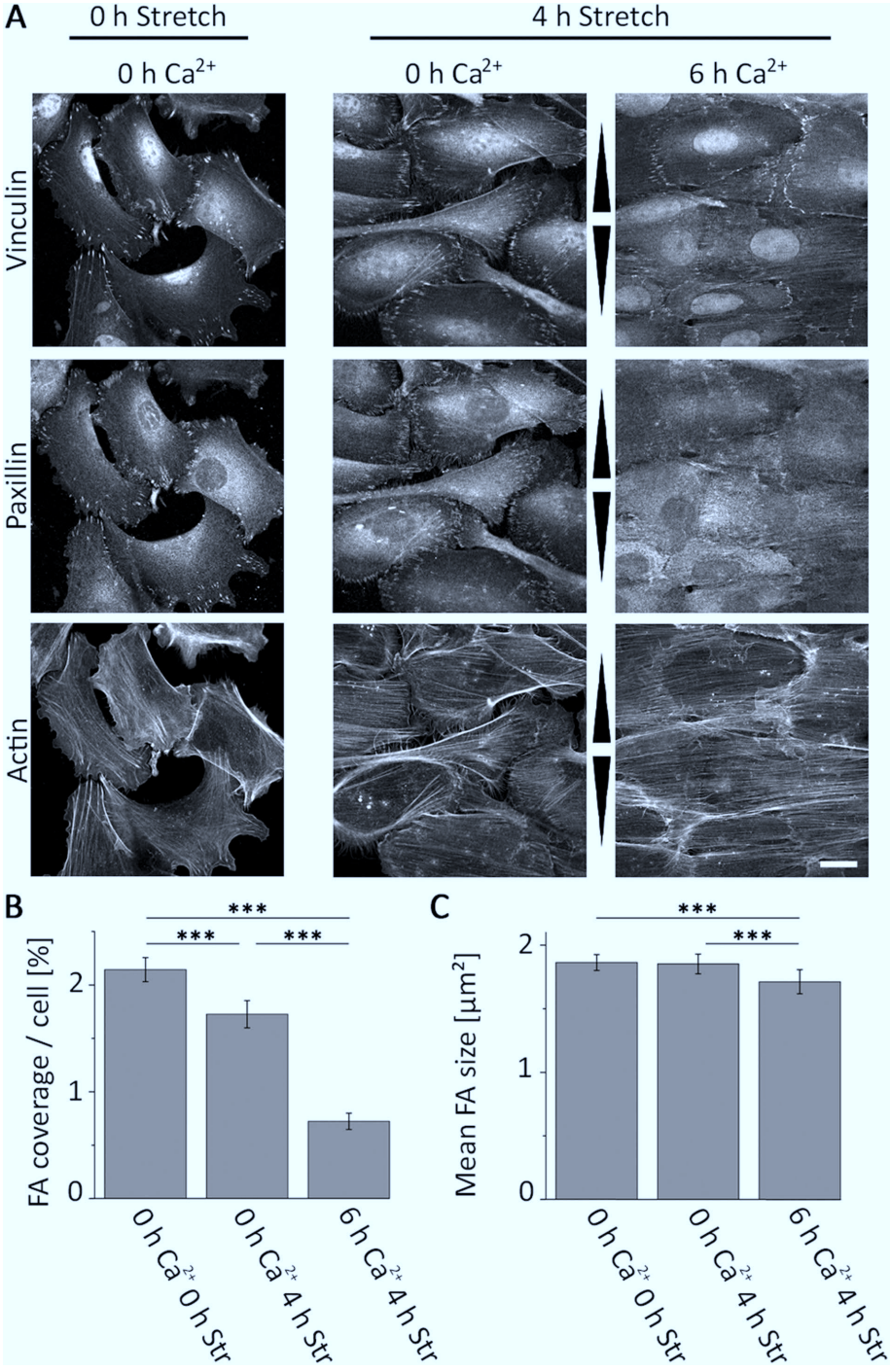

FIGURE 2: Straining of cell sheets induces loss of FAs. (A) Immunofluorescence micrograph for vinculin, paxillin, and actin of $Vinc^{Ctrl}$ cells after 0 and 4 h of cyclic stretch with different calcium incubation times (0 and 6 h). Arrowheads indicate stretch direction. Scale bar 20 µm. (B) Cell area covered with FAs and (C) mean FA size for different calcium incubation and stretching times are given ($n_{B\ 0\ h/0\ h} = 253$, $n_{B\ 0\ h/4\ h} = 238$, $n_{B\ 6\ h/4\ h} = 230$, $n_{C\ 0\ h/0\ h} = 253$, $n_{C\ 0\ h/4\ h} = 234$, $n_{C\ 6\ h/4\ h} = 208$).

more than 65% (Figure 2, A and B). These remaining FAs furthermore slightly decreased in size, while stretch in low calcium had no significant effect (Figure 2C). In contrast, vinculin incorporation into cell–cell contacts in high calcium medium remained unaffected by cyclic strain. These vinculin-positive structures were not costained with the FA marker paxillin, suggesting that AJs also form under cyclic stretch conditions. Furthermore, in contrast to predominantly cortical F-actin in the absence of stretch in high calcium, stretch induced formation of prominent, highly parallelized stress fibers that spanned the whole cell ending at cell–cell contacts on both ends. These F-actin fibers additionally showed a stronger perpendicular reorientation compared with those stretched in low calcium (Figure 2A; see also Supplemental Figure 2E).

FAs are largely dispensable for mechanosensation after cell–cell contact formation

On the basis of our observation of enhanced actin reorientation in response to strain for early cell sheets, we hypothesized that a further mechanosensitive machinery engaged on cell–cell contact formation. To investigate this, we impaired the FA-dependent mechanosensitive machinery using vinculin-deficient keratinocytes ($Vinc^{KO}$) for stretch experiments (Rubsam *et al.*, 2017). Actin filament orientations were equally distributed in the absence of strain in both control and $Vinc^{KO}$ cells cultured in low calcium (Figure 3, A, B, and E). In contrast, on stretching in low calcium media, stress fiber reorientation in $Vinc^{KO}$ cells was strongly reduced, indicating impaired FA-dependent mechanosensitivity (Figure 3, C and E). Under high calcium conditions, however, strain-induced actin reorientation was largely restored in $Vinc^{KO}$ cells to almost $Vinc^{Ctrl}$ levels (Figure 3, D and E). Restored reorientation took place only after cell-sheet formation, while high Ca^{2+} conditions on single cell level were unable to improve the impaired reorientation behavior of $Vinc^{KO}$ cells (Supplemental Figure 3). To confirm that the loss of vinculin indeed impaired stress-induced actin reorientaton through FAs, we knocked down the highly specific FA proteins paxillin and talin, respectively. mRNA levels were decreased to 40% (SD 6%) for paxillin and 10% (SD 10%) for talin ½, respectively (for protein knockdown efficiency see Supplemental Figure 4). Similarly to loss of vinculin, knockdown of paxillin induced a strongly impaired reorientation behavior in the absence of calcium but had no defect in stress-induced actin reorientation on calcium-induced AJ formation when compared with wild type (WT) (Figure 4, A, B, and E). Even more dramatic effects were found after knockdown of talin. Whereas talin-knockdown cells grown in low calcium were still able to adhere weakly in the absence of strain, these cells immediately lost contact on straining, accompanied by a complete loss of detectable actin bundles. In contrast, high Ca^{2+} restored their ability to respond to strain by forming cell-spanning stress fibers with reorientation angles similarly to those of control cells (Figure 4, C, D, and E).

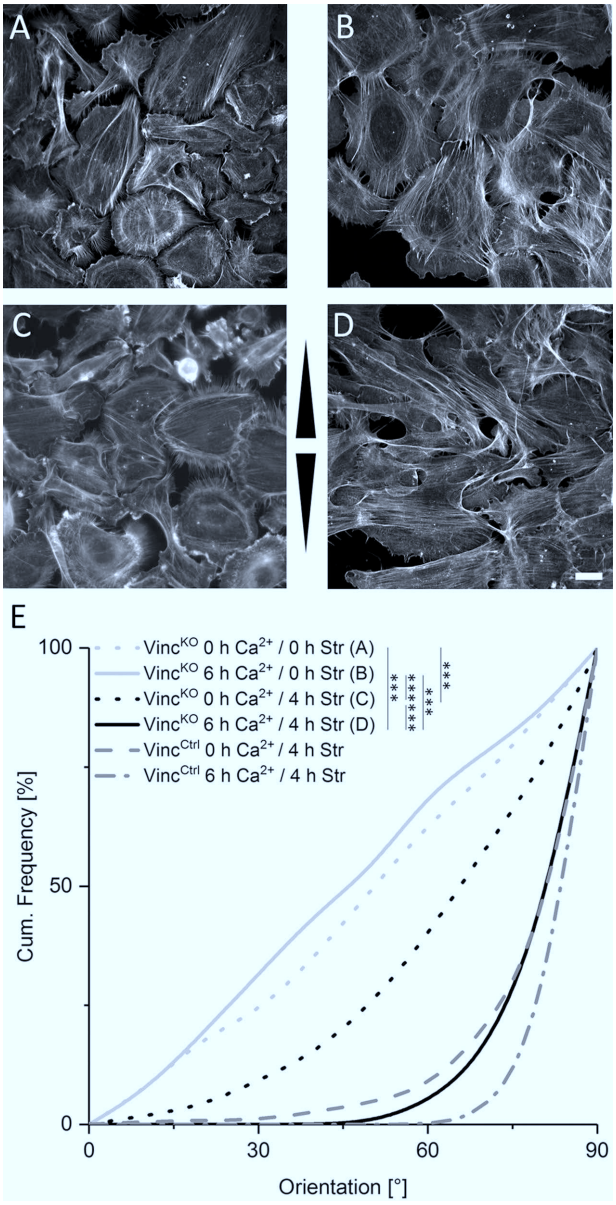

FIGURE 3: Actin fibers in cells with cell–cell contacts reorient independent on FAs. (A–D) Immunofluorescence micrographs of the actin network of Vinc^{KO} cells grown in the absence (A, C) or presence of calcium (B, D). For the last 4 h, cells remained either unstretched (A, B) or were stretched (C, D). Arrowheads indicate stretch direction. Scale bar 20 μm. (E) Cumulative histogram showing the angular distributions of actin fiber orientation for the respective experiments (no stretch: $n_{0h\ Ca^{2+}} = 368$ cells and $n_{6h\ Ca^{2+}} = 127$; stretch: $n_{0h\ Ca^{2+}} = 345$ and $n_{6h\ Ca^{2+}} = 224$). Angular distributions of actin fiber orientation in stretched Vinc^{Ctrl} cells are given for comparison.

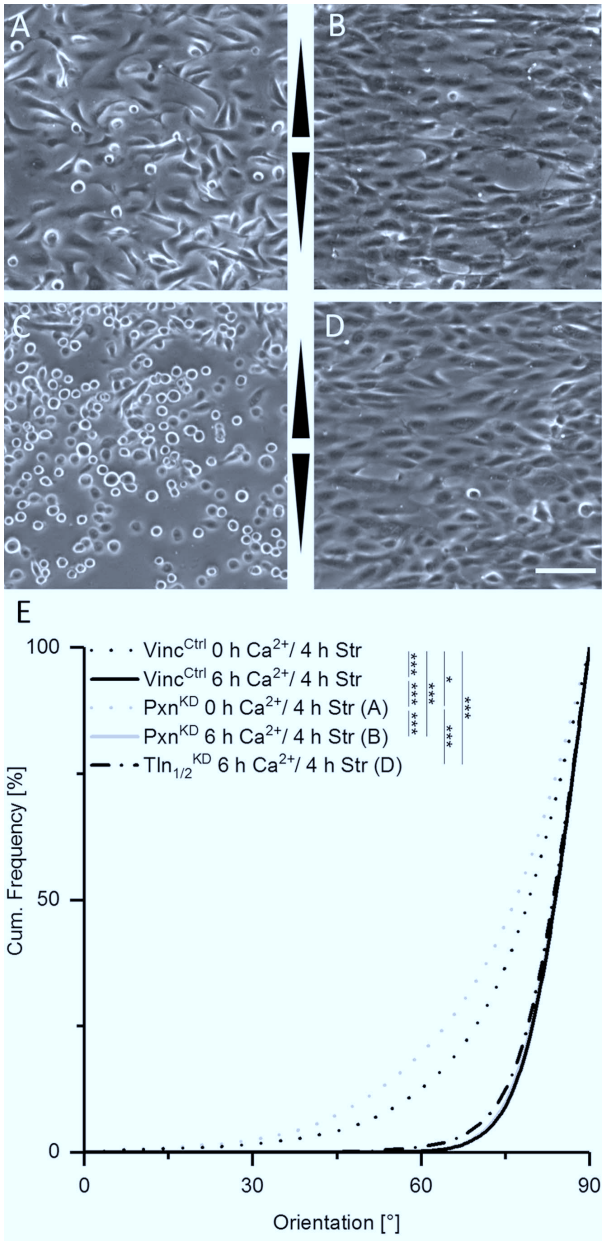

FIGURE 4: Loss of paxillin or talin impairs mechanosensitivity only in the absence of AJs. (A–D) Micrographs of paxillin knockdown (Pxn^{KD}, A, B) and talin knockdown (Tln^{KD}, C, D) cells in low calcium (A, C) and high calcium (B, D) after 4 h of stretching. Arrowheads indicate stretch direction. Scale bar 20 μm. (E) Cumulative histogram showing the angular distributions of actin fiber orientation for the respective experiments ($n_{PxnKD,\ 0\ h\ Ca^{2+}} = 1133$ cells and $n_{PxnKD,\ 6\ h\ Ca^{2+}} = 516$, $n_{Tln1/2KD,\ 6\ h\ Ca^{2+}} = 594$). WT (Vinc^{Ctrl}) distributions from Figure 3 are given for comparison.

Cell–cell contacts are responsible for enhanced fiber reorientation

We next directly addressed how AJs affect force-induced mechanosensation. We first used E-cadherin-deficient (ECad^{KO}) keratinocytes (Tunggal *et al.*, 2005), as this is the most abundant classical cadherin in these cells (Michels *et al.*, 2009). However, loss of E-cadherin did not obviously affect the stretch-induced F-actin reorientation response, regardless of whether these cells were allowed to form cell–cell junctions (high calcium) or not (low calcium) (Supplemental Figure 5).

Since P-cadherin is up-regulated in the absence of E-cadherin (Tunggal *et al.*, 2005; Tinkle *et al.*, 2008; Michels *et al.*, 2009) (Supplemental Figure 6), we next used ECad^{KO} keratinocytes additionally knocked down for P-cadherin (ECad^{KO}PCad^{KD}) (Michels *et al.*, 2009), which lack any detectable classical cadherins (Supplemental Figure 4A). Under low calcium conditions, ECad^{KO}PCad^{KD} responded similarly to strain as control keratinocytes, in agreement with our observation that FAs are the predominant mechanosensing element under these conditions. However, on allowing cells to form

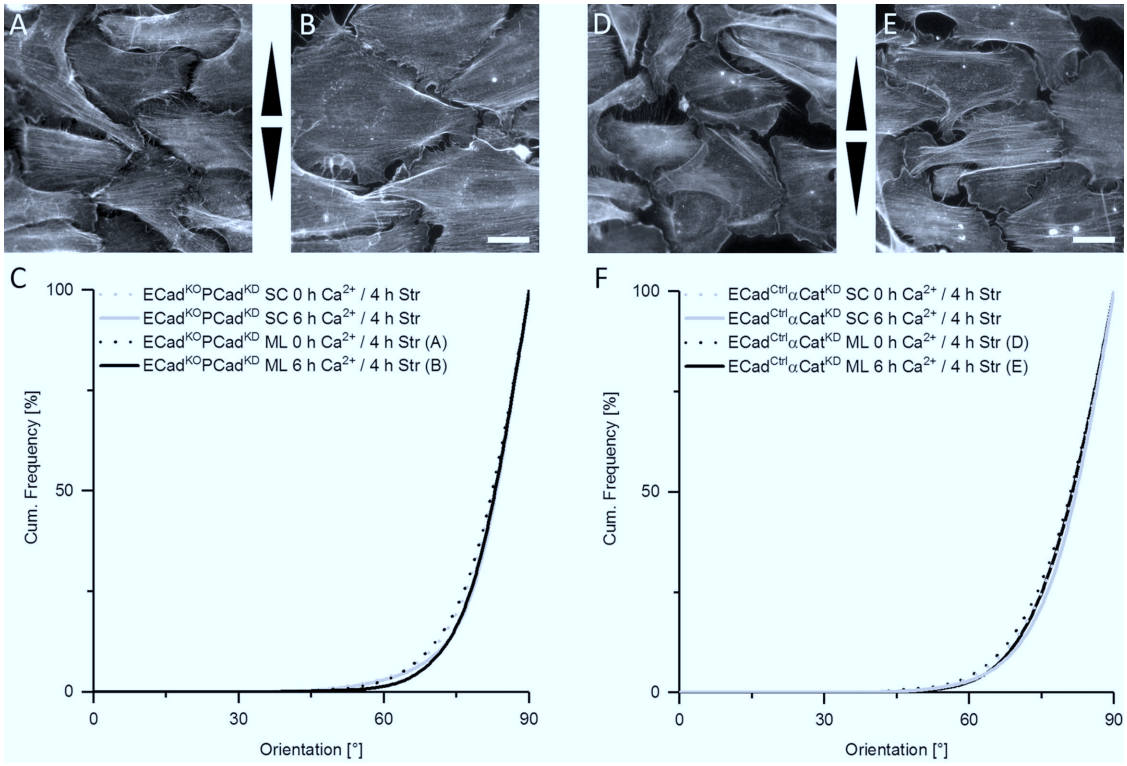

FIGURE 5: Increased actin fiber reorientation is based on AJs and α-catenin as mechanosensor. Immunofluorescence micrographs of the actin network after 4 h of stretch of $ECad^{KO}PCad^{KD}$ cells (A, B) and $ECad^{Ctrl}\alpha Cat^{KD}$ cells (D, E) grown in the absence (A, D) or presence of calcium (B, E). Arrowheads indicate stretch direction. Scale bar 20 µm. Cumulative histogram in C is showing the angular distributions of actin fiber orientation of $ECad^{KO}PCad^{KD}$ single cells (SC) and monolayers (ML) after 4 h of cyclic stretch without (n_{SC} = 277; n_{ML} = 432) and with calcium (n_{SC} = 270; n_{ML} = 421). In F the same cumulative histogram is given for stretched $ECad^{Ctrl}\alpha Cat^{KD}$ single and monolayer cells without (n_{SC} = 225; n_{ML} = 257) and in the presence of calcium (n_{SC} = 188; n_{ML} = 244). Note: Owing to AJ impairment all cells respond to strain just like single cells no matter if Ca^{2+} is present or not.

intercellular junctions for 6 h in high calcium, the reinforced actin reorientation seen in control cells is lost and the response remains identical to cells in low calcium conditions (Figure 5, A–C). Together, these data indicate that loss of AJs impairs early cell-sheet specific mechanosensitivity with FAs as the only functional mechanosensing structure and a response as seen for separated cells.

α-Catenin is essential for the mechanosensoric function of AJs

We next asked how AJs control external force-induced cytoskeletal reorientation. As the actin-binding protein α-catenin was already identified as a force-sensitive protein in AJs (Yonemura *et al.*, 2010), we used small interfering RNA (siRNA) to efficiently knock down α-catenin (mRNA knockdown 87%, SD 6%) (for protein knockdown efficiency see Supplemental Figure 4) in primary control mouse keratinocytes (αCat^{KD}). Knockdown of α-catenin strongly reduced the stretch-induced actin reorientation for cells grown in high calcium, which was now almost identical to cells under low calcium conditions or single cells, strongly indicating that on loss of α-catenin high calcium grown keratinocytes keep using FAs as the main mechanosensitive element in these cells (Figure 5, D–F). Thus, α-catenin is a central mechanosensor of external force in AJs to drive actin reorganization.

Since α-catenin is also necessary to recruit vinculin to AJs in high calcium (Yonemura *et al.*, 2010; Twiss and de Rooij, 2013; Yao *et al.*, 2014), we further investigated whether α-catenin cooperated with vinculin to reorganize actin. For this purpose, we used mouse αCat^{KD} cells and reexpressed human full-length α-catenin as well as an α-catenin mutant lacking the vinculin binding domain (ΔvinBD). While all genetic variants responded similarly as control cells to external force at low calcium (Figure 6A), formation of AJs at high calcium restored stress-induced actin reorganization in cells expressing human WT α-catenin. In contrast, expression of ΔvinBD α-catenin only partially restored actin reorientation (Figure 6A), thus indicating that α-catenin controls this response in part through vinculin.

Finally, we asked how impairing FA- and AJ-dependent mechanosensitivity would affect F-actin reorganization by knocking down α-catenin in $Vinc^{KO}$ cells ($Vinc^{KO}\alpha Cat^{KD}$). Here, reduced levels of α-catenin had no further effect in low calcium due to the fully FA-dependent mechanosensitivity for these conditions. In contrast, when cells were allowed to induce intercellular junction formation in high calcium we detected a strongly reduced actin reorientation in $Vinc^{KO}\alpha Cat^{KD}$ cells compared with $Vinc^{KO}$ cells only (Figure 6B). Taken together, our data identify an essential role for FAs and AJs in force-dependent cytoskeletal organization and redistribution and show that both vinculin and α-catenin are essential mechanosensors in keratinocytes.

DISCUSSION

Mechanosensation for FAs as well as AJs depends on their structural ability to bind to actin bundles (Zaidel-Bar *et al.*, 2007; Kanchanawong *et al.*, 2010; Yonemura *et al.*, 2010; Twiss and de Rooij, 2013).

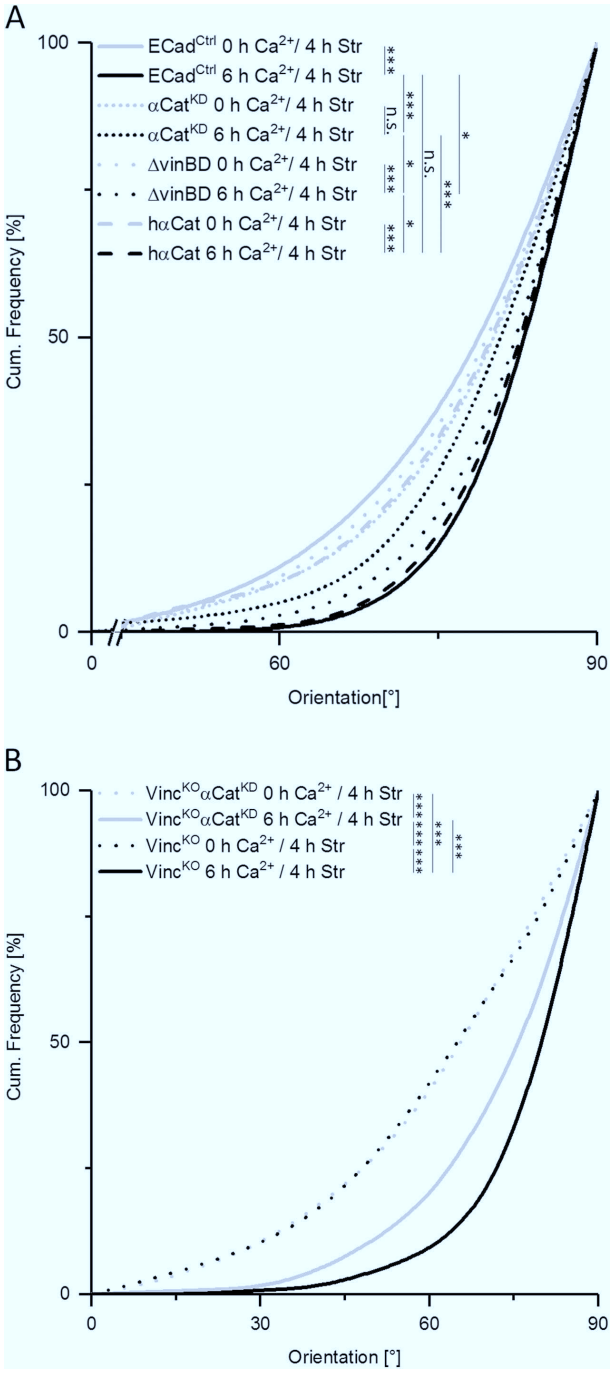

FIGURE 6: Mechanosensitivity of AJs depends on α-catenin and its binding partner, vinculin. Cumulative histogram showing the angular distributions of actin fiber orientation in WT keratinocytes ($Ecad^{Ctrl}$), cells treated with siRNA against endogenous mouse α-catenin (αCat^{KD}), and the same cells with reincorporated human α-catenin (hαCat) and human α-catenin lacking the vinculin binding domain (ΔvinBD). All cells were stretched for 4 h in the absence and presence (6 h) of high calcium ($n_{Ctrl\ 0\ h\ Ca^{2+}} = 416$; $n_{Ctrl\ 6\ h\ Ca^{2+}} = 305$; $n_{\alpha CatKD\ 0\ h\ Ca^{2+}} = 325$; $n_{\alpha CatKD\ 6\ h\ Ca^{2+}} = 451$; $n_{\Delta vinBD\ 0\ h\ Ca^{2+}} = 372$; $n_{\Delta vinBD\ 6\ h\ Ca^{2+}} = 763$; $n_{h\alpha Cat\ 0\ h\ Ca^{2+}} = 325$; $n_{h\alpha Cat\ 6\ h\ Ca^{2+}} = 662$). (B) Angular distributions of actin fiber orientation in $Vinc^{KO}\alpha Cat^{KD}$ cells with impaired FA- and AJ-dependent mechanosensitivity were plotted as cumulative histogram. Cells were stretched for 4 h in the absence or presence of calcium for 6 h ($n = 250$). Distributions of $Vinc^{KO}$ alone are given for comparison. Note the strongly reduced reorientation behavior of actin filaments in $Vinc^{KO}\alpha Cat^{KD}$ cells also for monolayer grown in high calcium.

While cell spanning actin bundles are present on the single-cell level in the absence and presence of strain, calcium-induced cell sheet formation leads to enhanced cortical actin localization and significant reduction of stress fibers (see also Supplemental Figure 3). Interestingly, cyclic strain dramatically induces cell spanning stress fiber formation even in cell sheets. Stress-induced actin bundles in cell sheets furthermore reorient almost perpendicular to strain direction and are additionally characterized by high order and reduced angular spread. Here, most likely cell cooperativity plays an important role, since AJs connect filaments between cells, leading to interdependencies of cytoskeletal orders within cell sheets (Lampugnani, 2010; Millan *et al.*, 2010). The reason for intense stress fiber formation in cell sheets remains elusive but this indicates that strain parameters used here exceed certain thresholds that already have be identified on a single-cell level (Chien, 2007). Furthermore, why stress fibers reorient to even higher angles in cell sheets than described for single cells (Faust *et al.*, 2011) is unclear.

As part of FA mechanosensitivity, manifold functions are described for vinculin (Carisey *et al.*, 2013; Case *et al.*, 2015) and largely depend on its ability to interact with various binding partners (Geiger and Bershadsky, 2001; Bakolitsa *et al.*, 2004; Ziegler *et al.*, 2006; Case *et al.*, 2015). However, vinculin is not the only molecule in FAs that affects stretch-induced F-actin reorganization, since paxillin or talin knockdown also had similar effects here, which argues for considerable changes in FA composition, maturation, or mechanosensitive force sensitivity in these cells (Humphries *et al.*, 2007). Interestingly, formation of AJs largely rescued loss of FA-dependent mechanosensitivity. Although various other types of cell–cell contacts are also present in epithelia, our data indicate the specific loss of mechanosensitivity for $ECad^{KO}PCad^{KD}$ cells. Both classical cadherins seem to complement each other regarding formation of mechanosensitive complexes as shown here for cells deleted for E-cadherin only. Our results fit well to other E-cadherin functions complemented by P-cadherin (Michels *et al.*, 2009).

On the molecular level, we showed that AJ-dependent mechanosensitivity is largely dependent on α-catenin as a mechanosensor with loss of cell-sheet specific responsiveness in the absence of α-catenin. The results fit well to data from other groups having described α-catenin as an important force-responsive molecule (Yonemura *et al.*, 2010; Twiss and de Rooij, 2013; Yao *et al.*, 2014). Interestingly, our data indicate that also its binding partner vinculin is important for AJ-dependent mechanosensitivity. These results are supported by magnetic twisting experiments showing that vinculin potentiates the E-cadherin mechanosensory response (le Duc *et al.*, 2010). Since AJ maturation additionally largely depends on applied forces (Huveneers *et al.*, 2012) and force-induced conformational unfolding of α-catenin allows vinculin binding in a 1:1 ratio (Yao *et al.*, 2014), mechanosensitive cooperativity of α-catenin and vinculin might be due to their ability to both bind to actin filaments.

In our experiments, we were not able to detect intensity differences for AJ-specific vinculin on strain application, although strain-induced incorporation of vinculin into cell–cell contacts had been described already (Thomas *et al.*, 2013). However, while detecting vinculin in high calcium at every cell–cell border in the absence of strain, we detected vinculin-comprising AJs on strain application preferentially at ends of reoriented stress fibers and therefore unequally distributed, which agrees well to the hypothesis of vinculin incorporation into active, force-bearing AJs (Yonemura *et al.*, 2010).

In summary, our experiments indicate that a functional mechanoperception exists in adhesive cells, no matter if such cell is separated or part of an interconnected cell sheet (see the model:

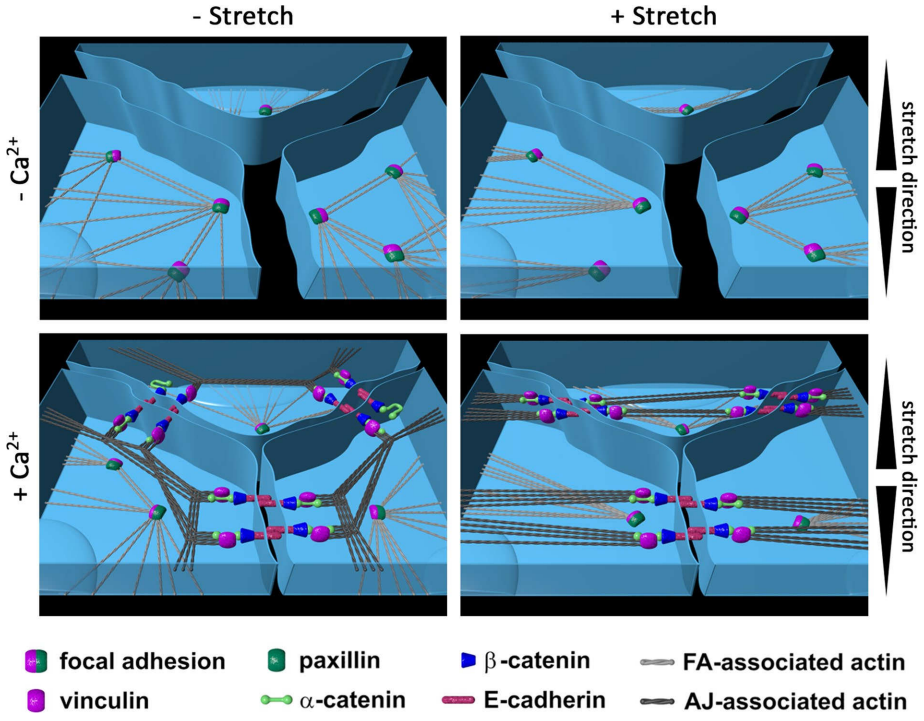

FIGURE 7: FA/AJ interplay model in mechanosensation. Keratinocytes in monolayers and low calcium conditions (top, left) are adhered via FAs to the substrate. Cell–cell contacts are barely formed. On stretching in low calcium medium (top, right) FAs function as mechanosensitive elements, causing stress fiber reorientation without changing FAs as main adhesion structure. Cells remain largely separated without forming zipperlike cell–cell contacts. In contrast, when cells are incubated in high calcium, epithelial sheet formation is induced (bottom, left) leading to zipperlike formation of AJs in apical cell regions and thereby reduced cell gaps, partial disassembly of FAs, incorporation of vinculin into AJs and actin filament relocalization to the cell periphery with contacts to AJs. On stretching of epithelial sheets (bottom, right), further FA disassembly takes place that is accompanied with translocation of mechanosensitive function from FAs to AJs. AJ-dependent strain recognition largely depends on α-catenin and attached vinculin and leads to highly parallelized actin filaments spanning the cells completely with angles being distributed sharply around perpendicular direction relative to strain and therefore higher angles than known for FA-dependent reorientations. For better visualization an animation is given as Supplemental Movie 1.

Figure 7 and Supplemental Movies 1–4). For epithelial cells, due to disassembly of FAs in suprabasal epithelial cell layers, mechanosensitivity translocates to newly formed AJs as further force bearing structure. Ultimately in response to stretch, FA as well as AJ-dependent mechanosensitivity induces reorientation of actin bundles away from applied stretch and causes cytoskeletal reinforcement bound to the respective adhesion complexes.

MATERIALS AND METHODS

Cell culture

Vinculin and E-cadherin-deficient cells were generated from epidermal, murine keratinocytes as described before (Michels *et al.*, 2009; Mertz *et al.*, 2013; Rubsam *et al.*, 2017). All cells were cultivated under sterile conditions at 32°C and 5% (vol/vol) CO_2 in low calcium (<0.5 mM) containing DMEM/Ham´s F12 medium (Biochrom, Berlin, Germany) supplemented with 10% FCS Gold (chelex treated) (PAA laboratories, Cölbe, Germany), 1% glutamine (Biochrom, Berlin, Germany), 1% penicillin/streptomycin (Biochrom, Berlin, Germany), 0.18 mM adenin (Sigma, St. Louis, MO), 0.5 µg/ml hydrocortisone (Sigma), 5 µg/ml insulin (Sigma), 10 ng/ml EGF (Sigma), 0.05 µg/µl choleratoxin (Sigma), and 5 µg/ml vitamin C (Sigma).

α-Catenin plasmids

For full-length α-catenin expression, αE-catenin was amplified from human cDNA and inserted into a pcDNA3 backbone. A 6-myc tag was amplified from pCS2+MT and inserted c-terminally of the α-catenin sequence. For ΔvinBD α-catenin, human αE-catenin cDNA fragments corresponding to the amino acids 1–200 and 377–906 were amplified and inserted into a pcDNA3 backbone including the c-terminal 6-myc tag.

RNAi experiments

siRNA was incorporated using Fuse-It-siRNA fusogenic liposomes (ibidi, Munich, Germany). $ECad^{Ctrl}$ cells and $Vinc^{KO}$ cells were fused for 12 min with siRNA directed against α-catenin 18 h after seeding of cells on six-well plates and again 24 h after first fusion. Twenty-four hours after second fusion, fused and untreated control cells were used for stretch experiments and determination of knockdown efficiency. Knockdown of paxillin and talin in $Vinc^{Ctrl}$ cells was performed using siRNAs against paxillin and talin 1 and talin 2 (Thermo Scientific, Waltham, MA), respectively. RNA isolation and cDNA generation was performed using RNeasy and a QuantiTect reverse transcription kit (Qiagen, Hilden, Germany) according to the manufacturer's protocols. Afterward, fusion efficiency was quantified by real-time PCR. Taq Man assays against α-catenin, paxillin, talin, and glyceraldehyde-3-phosphate dehydrogenase (GAPDH) as constitutively expressed marker (Qiagen, Hilden, Germany) were used. For reincorporation of human full-length α-catenin (h-αCat) and ΔvinBD α-catenin, cells were knocked down for endogenous α-catenin first by using a mouse-specific siRNA (siPOOL5; SiTools biotech, Martinsried, Germany). Four hours after siRNA treatment, α-catenin plasmids (full-length and ΔvinBD α-catenin) were incorporated using Viromer RED (Lipocalyx, Halle [Saale]). siRNA treatment and plasmid incorporation were repeated a second time after 24 h to guarantee high knockdown of endogenous α-catenin and sufficient expression of incorporated α-catenin versions. After further incubation for 24 h, cells were transferred to appropriate substrates for further analysis.

Western blot

Western blot analysis of crude protein extracts was performed according to Waschbüsch *et al.* (2009). Briefly, cells were harvested and lysed in lysis buffer (R0278; Sigma) supplemented with protease and phosphatase inhibitors (P8340, P0044, P5726; Sigma) for 30 min at 4°C. Protein extracts were heat inactivated, separated using 4–20% SDS–PAGE gels (Bio-Rad, Hercules, CA) and blotted to polyvinylidene difluoride (PVDF) membranes (Bio-Rad). Primary antibodies against tubulin (MAB1864; Merck, Darmstadt, Germany), paxillin (AH00492; Invitrogen, Carlsbad, CA), talin (sc-15336; Santa Cruz Biotechnology, Dallas, TX), α-catenin (C2081; Sigma), c-Myc (M5546; Sigma) and E-cadherin (610182; BD Bioscience, Franklin Lakes, NJ) were used and detected by alkaline

phosphatase (ALP)-coupled secondary antibodies directed against rat, rabbit, and mouse (Sigma), respectively.

Elastic substrate preparation

Elastic silicone chambers for stretch experiments were prepared and calibrated as described previously (Faust *et al*., 2011). To mimic elasticities of the basement membrane in vivo (Tilleman *et al*., 2004; Pawlaczyk *et al*., 2013), elasticities were set to 50 kPa. Chambers were coated with fibronectin (20 µg/ml) in PBS for 1 h at 37°C prior to cell seeding. Since $Vinc^{KO}$ cells were smaller by 30% on average, cell numbers were adapted to ensure identical conditions during monolayer formation (28,000 cells/cm^2 for $Vinc^{KO}$ and $Vinc^{KO}$ αCat^{KD} cells and 21,000 cells/cm^2 for all other cell types).

Cell straining

Before initiation of cyclic stretch, cells seeded on elastic chambers were incubated with 1.8 mM Ca^{2+} containing media for 2 h and were kept in high calcium media throughout the experiment. Control cells were kept in low calcium cultivation media (<0.5 mM Ca^{2+}). A linear stage for simultaneous, uniaxial stretch of six chambers was used for the experiments (adapted from single chamber stretcher previously described in Faust *et al*. [2011]). Cells were stretched for 4 h with 300 mHz and 14%. For focal adhesion analyses, 1.8 mM Ca^{2+} was added to the cells for 2, 6, and 24 h. Control cells were kept in low calcium media.

Immunocytochemistry

Immunocytochemistry experiments were performed as described earlier (Faust *et al*., 2011). Primary antibodies used were anti-vinculin from mouse (V9131; Sigma), anti-vinculin from rabbit (700062; Invitrogen, Carlsbad, CA), anti-paxillin from mouse (AH00492; CellSignaling, Cambridge, UK), and anti-E-cadherin from mouse (610182; BD Bioscience, San José, CA). Alexa Fluor 488 anti-rabbit from chicken (A21441; Life Technologies, Carlsbad, CA), Alexa Fluor 488 anti-mouse from chicken (A21200; Life Technologies, Carlsbad, CA), Alexa Fluor 633 anti-rabbit from goat (A21071; Life Technologies), and Alexa Fluor 633 anti-mouse from goat (A21126; Life Technologies) were used as secondary antibodies. Actin was stained with Alexa Fluor 546 phalloidin (A22283; Life Technologies) and Alexa Fluor 488-i phalloidin (U0281; Abnova, Taipei City, Taiwan).

Microscopy

Adhesion proteins were analyzed on a confocal laser scanning microscope (LSM 710; Carl Zeiss, Jena, Germany) with a 40× EC-PlanNeofluar/Ph3/1.3 NA oil immersion objective using appropriate settings for excitation and emission. Images for the analysis of actin fiber orientation were done using a widefield microscope (AxioObserver; Carl Zeiss) equipped with a 40× EC-PlanNeofluar/Ph3/1.3 NA oil immersion objective (Carl Zeiss).

Analysis of actin fiber orientation

The analysis of actin fiber orientation was based on the structure tensor approach described in Faust *et al*. (2011). Here, we manually marked individual cells and excluded the thick fibers encircling the cell. In the inner area, local fiber orientations were determined from gray value gradients. Main actin fiber orientation was determined as the maximum of the distribution of angles within the cell area (parabola fit for suppression of noise).

Detection of focal adhesions

To detect FAs, cells were manually separated on images stained for paxillin. Subsequently, an algorithm described in Hersch *et al*. (2013) was used. In brief, images were bandpass-filtered (9 × 9 binomial filter and 45 × 45 binomial filter subtracted; pixel size 94 nm). Average and SD were determined for each pixel in a 45-pixel-wide square centered on it. Pixels with a z-score (difference of pixel value and local mean divided by local SD) exceeding 1 were chosen as candidates. Only connected regions of sizes between 45 and 1000 pixels were considered. FAs with low contrast to their neighborhood were rejected.

Colocalization analysis

For this analysis, whole images of paxillin and vinculin staining were used. As a preprocessing step, the images were Gaussian filtered (two-dimensional Gaussian smoothing kernel with SD of 0.5, pixel size 94 nm). Then FAs were detected in both channels as described above, and overlapping FA areas in the paxillin and vinculin images were determined.

Determination of actin localization parameter

In a first step, all analyzed actin-labeled cells were marked manually. Then each marked cell was transformed to the unit circle with a radius of 200 pixels as described in Mohl *et al*. (2012). This unit cell was subdivided into evenly spaced concentric rings, all with a width of five pixel followed by average gray value calculation for each ring. Then a straight line was fitted to the average gray values. The actin localization parameter was defined as the slope of this line. Positive values indicate high actin concentration in the cellular periphery compared with its center and vice versa.

Statistical analysis

The Wilcoxon test was used for determination of statistical significance (upper limits: $*p = 0.05$, $**p = 0.01$, $***p = 0.005$). Detailed statistical information for all experiments is given in Supplemental Figure 1.

ACKNOWLEDGMENTS

This work received funding from the European Union's Horizon 2020 research and innovation program under Marie Sklodowska-Curie grant agreement No. 642866. It was also supported by the Deutsche Forschungsgemeinschaft (Schwerpunktprogramm SPP1782).

REFERENCES

Bakolitsa C, Cohen DM, Bankston LA, Bobkov AA, Cadwell GW, Jennings L, Critchley DR, Craig SW, Liddington RC (2004). Structural basis for vinculin activation at sites of cell adhesion. Nature 430, 583–586.

Braga VMM, Hodivala KJ, Watt FM (2009). Calcium-induced changes in distribution and solubility of cadherins, integrins and their associated cytoplasmic proteins in human keratinocytes. Cell Commun Adhes 3, 201–215.

Carisey A, Tsang R, Greiner AM, Nijenhuis N, Heath N, Nazgiewicz A, Kemkemer R, Derby B, Spatz J, Ballestrem C (2013). Vinculin regulates the recruitment and release of core focal adhesion proteins in a force-dependent manner. Curr Biol 23, 271–281.

Case LB, Baird MA, Shtengel G, Campbell SL, Hess HF, Davidson MW, Waterman CM (2015). Molecular mechanism of vinculin activation and nanoscale spatial organization in focal adhesions. Nat Cell Biol 17, 880–892.

Chien S (2007). Mechanotransduction and endothelial cell homeostasis: the wisdom of the cell. Am J Physiol Heart Circ Physiol 292, H1209–H1224.

Chuong CM, Nickoloff BJ, Elias PM, Goldsmith LA, Macher E, Maderson PA, Sundberg JP, Tagami H, Plonka PM, Thestrup-Pedersen K, *et al*. (2002). What is the "true" function of skin? Exp Dermatol 11, 159–187.

del Rio A, Perez-Jimenez R, Liu R, Roca-Cusachs P, Fernandez JM, Sheetz MP (2009). Stretching single talin rod molecules activates vinculin binding. Science 323, 638–641.

Eckert RL (1989). Structure, function, and differentiation of the keratinocyte. Physiol Rev 69, 1316–1346.

Faust U, Hampe N, Rubner W, Kirchgessner N, Safran S, Hoffmann B, Merkel R (2011). Cyclic stress at mHz frequencies aligns fibroblasts in direction of zero strain. PLoS One 6, e28963.
Fuchs E (1990). Epidermal differentiation: the bare essentials. J Cell Biol 111, 2807–2814.
Geiger B, Bershadsky A (2001). Assembly and mechanosensory function of focal contacts. Curr Opin Cell Biol 13, 584–592.
Hayakawa K, Hosokawa A, Yabusaki K, Obinata T (2000). Orientation of smooth muscle-derived A10 cells in culture by cyclic stretching: relationship between stress fiber rearrangement and cell reorientation. Zoolog Sci 17, 617–624.
Hayakawa K, Sato N, Obinata T (2001). Dynamic reorientation of cultured cells and stress fibers under mechanical stress from periodic stretching. Exp Cell Res 268, 104–114.
Herman B, Harrington MA, Olashaw NE, Pledger WJ (1986). Identification of the cellular mechanisms responsible for platelet-derived growth factor induced alterations in cytoplasmic vinculin distribution. J Cell Physiol 126, 115–125.
Hersch N, Wolters B, Dreissen G, Springer R, Kirchgessner N, Merkel R, Hoffmann B (2013). The constant beat: cardiomyocytes adapt their forces by equal contraction upon environmental stiffening. Biol Open 2, 351–361.
Hodivala KJ, Watt FM (1994). Evidence that cadherins play a role in the downregulation of integrin expression that occurs during keratinocyte terminal differentiation. J Cell Biol 124, 589–600.
Humphries JD, Wang P, Streuli C, Geiger B, Humphries MJ, Ballestrem C (2007). Vinculin controls focal adhesion formation by direct interactions with talin and actin. J Cell Biol 179, 1043–1057.
Huveneers S, Oldenburg J, Spanjaard E, van der Krogt G, Grigoriev I, Akhmanova A, Rehmann H, de Rooij J (2012). Vinculin associates with endothelial VE-cadherin junctions to control force-dependent remodeling. J Cell Biol 196, 641–652.
Jungbauer S, Gao H, Spatz JP, Kemkemer R (2008). Two characteristic regimes in frequency-dependent dynamic reorientation of fibroblasts on cyclically stretched substrates. Biophys J 95, 3470–3478.
Kanchanawong P, Shtengel G, Pasapera AM, Ramko EB, Davidson MW, Hess HF, Waterman CM (2010). Nanoscale architecture of integrin-based cell adhesions. Nature 468, 580–584.
Lampugnani MG (2010). Endothelial adherens junctions and the actin cytoskeleton: an "infinity net"? J Biol 9, 16.
le Duc Q, Shi Q, Blonk I, Sonnenberg A, Wang N, Leckband D, de Rooij J (2010). Vinculin potentiates E-cadherin mechanosensing and is recruited to actin-anchored sites within adherens junctions in a myosin II-dependent manner. J Cell Biol 189, 1107–1115.
Mertz AF, Che Y, Banerjee S, Goldstein JM, Rosowski KA, Revilla SF, Niessen CM, Marchetti MC, Dufresne ER, Horsley V (2013). Cadherin-based intercellular adhesions organize epithelial cell-matrix traction forces. Proc Natl Acad Sci USA 110, 842–847.
Michels C, Buchta T, Bloch W, Krieg T, Niessen CM (2009). Classical cadherins regulate desmosome formation. J Invest Dermatol 129, 2072–2075.
Millan J, Cain RJ, Reglero-Real N, Bigarella C, Marcos-Ramiro B, Fernandez-Martin L, Correas I, Ridley AJ (2010). Adherens junctions connect stress fibres between adjacent endothelial cells. BMC Biol 8, 11.
Miroshnikova YA, Le HQ, Schneider D, Thalheim T, Rubsam M, Bremicker N, Polleux J, Kamprad N, Tarantola M, Wang I, *et al.* (2018). Adhesion forces and cortical tension couple cell proliferation and differentiation to drive epidermal stratification. Nat Cell Biol 20, 69–80.
Mohl C, Kirchgessner N, Schafer C, Hoffmann B, Merkel R (2012). Quantitative mapping of averaged focal adhesion dynamics in migrating cells by shape normalization. J Cell Sci 125, 155–165.
Neidlinger-Wilke C, Grood E, Claes L, Brand R (2002). Fibroblast orientation to stretch begins within three hours. J Orthop Res 20, 953–956.
O'Keefe EJ, Briggaman RA, Herman B (1987). Calcium-induced assembly of adherens junctions in keratinocytes. J Cell Biol 105, 807–817.
Opas M, Turksen K, Kalnins VI (1985). Adhesiveness and distribution of vinculin and spectrin in retinal pigmented epithelial cells during growth and differentiation in vitro. Dev Biol 107, 269–280.
Pawlaczyk M, Lelonkiewicz M, Wieczorowski M (2013). Age-dependent biomechanical properties of the skin. Postępy Dermatol Alergol 30, 302–306.
Rubsam M, Mertz AF, Kubo A, Marg S, Jungst C, Goranci-Buzhala G, Schauss AC, Horsley V, Dufresne ER, Moser M, *et al.* (2017). E-cadherin integrates mechanotransduction and EGFR signaling to control junctional tissue polarization and tight junction positioning. Nat Commun 8, 1250.
Rudiger M (1998). Vinculin and alpha-catenin: shared and unique functions in adherens junctions. Bioessays 20, 733–740.
Sanders JE, Goldstein BS, Leotta DF (1995). Skin-response to mechanical-stress—adaptation rather than breakdown: a review of the literature. J Rehabil Res Dev 32, 214–226.
Sawada Y, Tamada M, Dubin-Thaler BJ, Cherniavskaya O, Sakai R, Tanaka S, Sheetz MP (2006). Force sensing by mechanical extension of the Src family kinase substrate p130Cas. Cell 127, 1015–1026.
Simpson CL, Patel DM, Green KJ (2011). Deconstructing the skin: cytoarchitectural determinants of epidermal morphogenesis. Nat Rev Mol Cell Biol 12, 565–580.
Thomas WA, Boscher C, Chu YS, Cuvelier D, Martinez-Rico C, Seddiki R, Heysch J, Ladoux B, Thiery JP, Mege RM, Dufour S (2013). alpha-Catenin and vinculin cooperate to promote high E-cadherin-based adhesion strength. J Biol Chem 288, 4957–4969.
Tilleman TR, Tilleman MM, Neumann MH (2004). The elastic properties of cancerous skin: Poisson's ratio and Young's modulus. Isr Med Assoc J 6, 753–755.
Tinkle CL, Pasolli HA, Stokes N, Fuchs E (2008). New insights into cadherin function in epidermal sheet formation and maintenance of tissue integrity. Proc Natl Acad Sci USA 105, 15405–15410.
Tunggal JA, Helfrich I, Schmitz A, Schwarz H, Gunzel D, Fromm M, Kemler R, Krieg T, Niessen CM (2005). E-cadherin is essential for in vivo epidermal barrier function by regulating tight junctions. EMBO J 24, 1146–1156.
Twiss F, de Rooij J (2013). Cadherin mechanotransduction in tissue remodeling. Cell Mol Life Sci 70, 4101–4116.
Vaezi A, Bauer C, Vasioukhin V, Fuchs E (2002). Actin cable dynamics and Rho/Rock orchestrate a polarized cytoskeletal architecture in the early steps of assembling a stratified epithelium. Dev Cell 3, 367–381.
Vasioukhin V, Bauer C, Yin M, Fuchs E (2000). Directed actin polymerization is the driving force for epithelial cell–cell adhesion. Cell 100, 209–219.
Wang JH, Goldschmidt-Clermont P, Wille J, Yin FC (2001). Specificity of endothelial cell reorientation in response to cyclic mechanical stretching. J Biomech 34, 1563–1572.
Waschbüsch D, Born S, Niediek V, Kirchgessner N, Tamboli IY, Walter J, Merkel R, Hoffmann B (2009). Presenilin 1 affects focal adhesion site formation and cell force generation via c-Src transcriptional and posttranslational regulation. J Biol Chem 284, 10138–10149.
Yao M, Qiu W, Liu R, Efremov AK, Cong P, Seddiki R, Payre M, Lim CT, Ladoux B, Mege RM, Yan J (2014). Force-dependent conformational switch of alpha-catenin controls vinculin binding. Nat Commun 5, 4525.
Yonemura S, Wada Y, Watanabe T, Nagafuchi A, Shibata M (2010). alpha-Catenin as a tension transducer that induces adherens junction development. Nat Cell Biol 12, 533–542.
Zaidel-Bar R, Itzkovitz S, Ma'ayan A, Iyengar R, Geiger B (2007). Functional atlas of the integrin adhesome. Nat Cell Biol 9, 858–867.
Ziegler WH, Liddington RC, Critchley DR (2006). The structure and regulation of vinculin. Trends Cell Biol 16, 453–460.